SpaceChargeLimited Currents in Organic Crystals

Peter Mark and Wolfgang Helfrich

Citation: Journal of Applied Physics **33**, 205 (1962); doi: 10.1063/1.1728487
View online: http://dx.doi.org/10.1063/1.1728487
View Table of Contents: http://scitation.aip.org/content/aip/journal/jap/33/1?ver=pdfcov
Published by the AIP Publishing

Space-Charge-Limited Currents in Organic Crystals*

PETER MARK†
Research Division, Polaroid Corporation, Cambridge, Massachusetts

AND

WOLFGANG HELFRICH
Laboratorium für Technische Physik, Technische Hochschule, München, Germany

(Received May 18, 1961)

Electrical conductivity measurements were performed with thin (50 μ) single crystals of *p*-terphenyl, *p*-quaterphenyl, and anthracene supplied with aqueous electrodes, one of which was an iodine-iodide solution (acceptor electrode), and the other an iodide solution. The results strongly indicate that the acceptor electrode can form ohmic contact for hole injection into these crystals and that space-charge-limited currents can be drawn through them. The crystals were found to contain hole-trapping states the location-in-energy of which can be approximated by a decreasing exponential distribution above the valence band. The measurements showed that the hole mobility in *p*-terphenyl is about 3×10^{-2} cm²/v sec, is independent of the field at least up to about 4×10^{4} v/cm, and that the hole-trap concentration is at least 10^{13} cm^{-3}. The acceptor electrode used does not form ohmic contact to crystals of naphthalene and diphenyl; an explanation for this is proposed. Some theoretical aspects of ohmic contact formation to organic crystals and space-charge-limited current flow in insulators are also discussed.

I. INTRODUCTION

CURRENT flow through an insulator is limited by space-charge when carriers in excess of those present in thermal equilibrium can be injected through an ohmic contact. Rose[1] and Lampert[2] have shown that space-charge-limited current measurements are a sensitive tool for determining the carrier mobility and the concentration and energy distribution of carrier trapping states. The experimental detection of space-charge-limited current flow in CdS by Smith and Rose[3] and in ZnS by Ruppel[4] was facilitated by the ability of certain electrode metals (e.g., indium and gallium) to form ohmic contact to these insulators.[5] Recently, the nature of electrode contacts to organic crystals has also come under investigation. In particular, Kallmann and Pope[6,7] have used a saturated solution of iodine in 1.0 *M* NaI as an acceptor electrode to inject positive holes into single crystals of anthracene, and Boroffka[8] has reported that a solid solution of iodine in CuI, used as an electrode, can also supply holes to the same material.

In this paper, we shall discuss the results of a series of experiments with thin single crystals of diphenyl, *p*-terphenyl, *p*-quaterphenyl, naphthalene, and anthracene. We will show: (1) that the acceptor electrode of Kallmann and Pope can form ohmic contact for hole injection to crystals of the above compounds with more than 2 rings per molecule, (2) that the steady-state current through such crystals is trap-limited space-charge-limited so long as the injecting contact is ohmic, and that the hole current saturates above a certain current level when the ohmic nature of the contact is destroyed because of carrier exhaustion in the electrode, and (3) that the initial transient current can approach trap-free space-charge-limited current flow. We also obtain the mobility of holes in *p*-terphenyl and estimate the volume concentration and the form of the distribution in energy above the valence band of the hole-trapping states.

In the Appendix, we discuss the details of the current transient measurements and derive the pertinent formulas relating to space-charge-limited current flow in insulators. We also show that the error introduced by neglecting the diffusive contribution to the total current in the calculations is small. All calculations are based on a one-dimensional plane geometry, and the equations are written in mks units.

II. INSTRUMENTATION

Single crystals of diphenyl, *p*-terphenyl, *p*-quaterphenyl, napthlene, and anthracene were grown from the vapor phase under dry nitrogen at atmospheric pressure. Zone-refined chemical grade materials were used. The crystals were all transparent colorless platelets about 50 μ thick and up to 4 cm² in area. The anthracene contained traces of tetracene which were not removed by zone refining. This impurity gave rise to a strong green component in the fluorescence spectrum and extended the absorption spectrum for photoconductivity well into the visible range ($\lambda>4000$ A).[9]

The measurements were made with the crystals

* A preliminary account was presented at the meeting of the Bavarian Physical Society, Würzburg, April 25–26, 1961.

† On leave at the Laboratorium für Technische Physik, Technische Hochschule, München, during the academic year 1960–1961.

[1] A. Rose, Phys. Rev. **97**, 1538 (1955).
[2] M. A. Lampert, Phys. Rev. **103**, 1648 (1956).
[3] R. W. Smith and A. Rose, Phys. Rev. **97**, 1531 (1955).
[4] W. Ruppel, Helv. Phys. Acta **31**, 311 (1958).
[5] R. W. Smith, Phys. Rev. **97**, 1525 (1955); and F. A. Kröger, G. Diemer, and H. A. Klasens, Phys. Rev. **103**, 279 (1956).
[6] H. Kallmann and M. Pope, J. Chem. Phys. **32**, 300 (1960).
[7] H. Kallmann and M. Pope, Nature **186**, 31 (1960).
[8] H. Boroffka, Z. Physik **160**, 93 (1960).
[9] C. G. B. Garrett in *Semiconductors*, edited by N. B. Hanney (Reinhold Publishing Corporation, New York, 1959), Chap. 15, pp. 643–675.

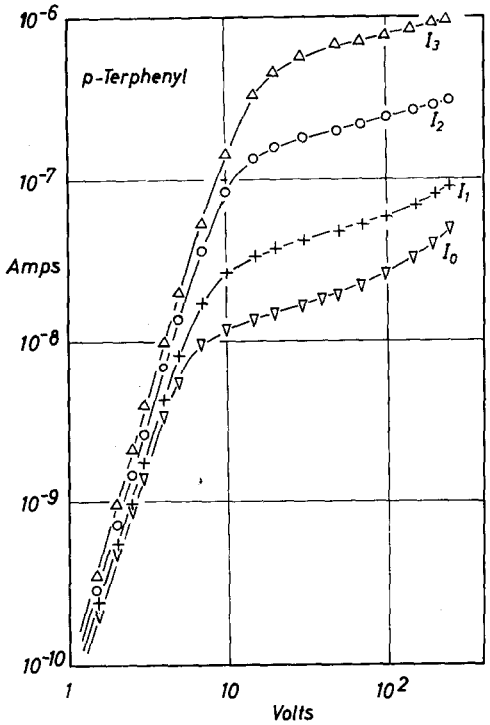

FIG. 1. Forward steady-state current-voltage characteristic of p-terphenyl. I_0 is the dark current, and I_1, I_2, and I_3 are the currents obtained under illumination with the band S_2 ($\lambda > 5100$ A). The subscripts 1, 2, and 3 indicate increasing intensity in that order.

mounted in a holder similar to that used by Kallmann and Pope.[10] The electrode contact area was 0.25 cm^2, and the leakage resistance was greater than 10^{15} ohms. A light source (200-w tungsten bulb operated at a color temperature of 3075°K) was situated so that appropriately filtered light could be made incident through the NaI electrode and the crystal onto the acceptor electrode. Two spectral bands were used: S_1 with 3600 A$<\lambda<$6000 A and S_2 with $\lambda>5100$ A. The intensity was varied by interposing wire mesh screens in the path of the light. The maximum intensity at the position of the crystal was about 0.5 milliwatts/cm^2.

The current measuring system included a regulated variable dc power supply (generating from 0.1 to 600 v) in series with the crystal and a Keithly 610 micro-microammeter and dc amplifier, the output of which was fed into a Tektronix 502 double-beam oscilloscope. The equivalent circuit can be pictured as a series combination of 2 impedances Z_m and Z_c, the first of which represents the ammeter and the second the crystal. Both Z_m and Z_c can further be represented as a parallel combination of a resistance and a capacitance R_m, C_m and R_c, C_c, respectively. R_m is the resistance of the ammeter across which the voltage drop was measured to obtain the current through R_c, which is the voltage-dependent resistance [see Eqs. (2) and (4)] of the crystal. Hence $R_m \ll R_c$. C_m is the combined input capacitance of the ammeter and the cable capacitance, and C_c is the capacitance of the crystal. For our circuit C_m and $C_c \simeq 10^{-10}$ farads. The voltage source in series with this circuit had a rise time $\tau_s \simeq 2\times10^{-4}$ sec (see the voltage trace of Fig. 4). The entire circuit was encased in a grounded metal box which served as an adequate shield from electrical pick-up.

[10] H. Kallmann and M. Pope, Rev. Sci. Instr. **30**, 1548 (1959).

III. RESULTS

A. Steady-State Current Measurements

A typical forward steady-state current voltage characteristic (with the acceptor electrode at positive bias) obtained from a p-terphenyl crystal is illustrated in Fig. 1. The curve labeled I_0 is the dark current, and the curves I_1, I_2, and I_3 are the currents obtained when the acceptor electrode is illuminated with the band S_2. The subscripts 1, 2, and 3 indicate increasing intensity in that order. Each curve exhibits 2 distinct regions—a steep portion at lower voltages followed by a saturation region at higher voltages. In the steep region, the current varies as the cube of the voltage and increases only slightly with increasing intensity. The saturation current is strongly photosensitive. The slight increase in the dark current at the high voltage end of the curve is probably due to the onset of break-down since the current was rather noisy.

Current-voltage curves obtained with the same crystal under illumination with various intensities in the band S_1 had a similar appearance and hence are not shown. In the steep portion, the current again varied with the cube of the voltage, and the saturation current increased with the decreasing penetration depth of the shorter wavelength radiation into the acceptor electrode from the crystal-electrode interface.

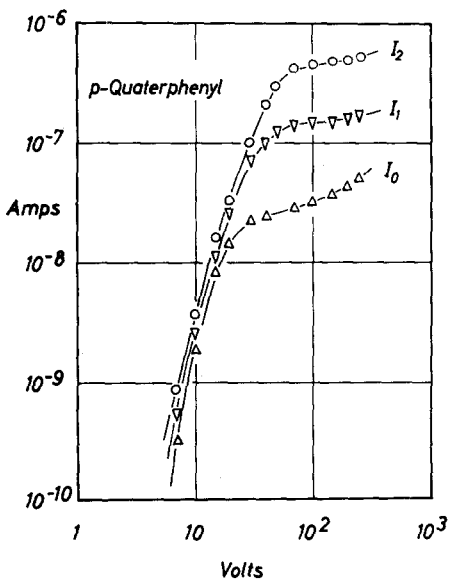

FIG. 2. Forward steady-state current-voltage characteristic of p-quaterphenyl. I_0 is the dark current, and I_1 and I_2 are the currents obtained under illumination with the band S_2.

The reverse dark current (with the acceptor electrode at negative bias) was always less than 10^{-10} amp. No noticeable current enhancement was measured when the crystal-electrode combination was exposed to radiation in either band S_1 or S_2. This was also so when pure 1.0 M NaI solutions were used on both sides of the crystal.

The forward current-voltage characteristic obtained with a p-quaterphenyl crystal is illustrated in Fig. 2. Curve I_0 is the dark current, and curves I_1 and I_2 were obtained under illumination with the band S_2 (I_2 of this figure and I_3 of Fig. 1 were measured at the same intensity). These curves are similar to those of Fig. 1 except that the slope in the steep portion of each curve is not strictly constant. To a first approximation, however, the slope is about 3. A change in the spectral distribution of the exciting radiation to S_1 influences the current-voltage curves in the same way as it does those of p-terphenyl, and the reverse current was also less than 10^{-10} amp.

A similar experiment was also performed with an anthracene crystal. The results are shown in Fig. 3. Curve I_0 is the dark current which is roughly proportional to V^{12}, and I_1 is the current obtained under illumination with the band S_1. The current I_1 is much larger than I_0 in the steep portion and does not follow a power-law relation with the voltage. Since this crystal became photoconducting in the band S_1 with pure 1.0 M NaI on both sides of the crystal, some of the carriers contributing to the current I_1 are the result of photo-

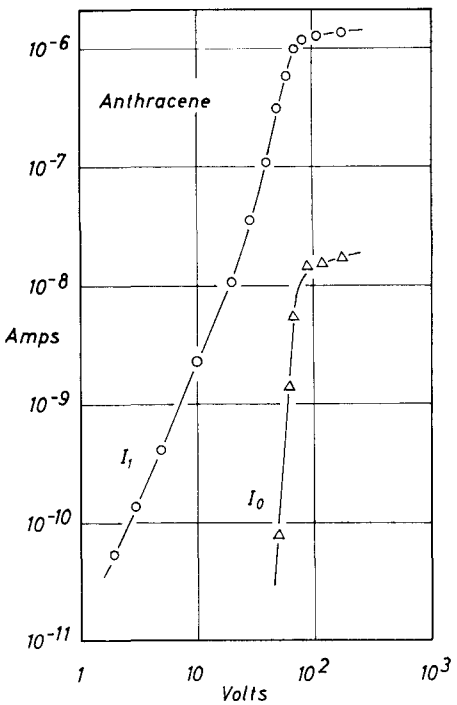

FIG. 3. Forward steady-state current-voltage characteristic of anthracene. I_0 is the dark current, and I_1 is the current obtained under illumination with the band S_1 (3600 A $<\lambda<$ 4000 A).

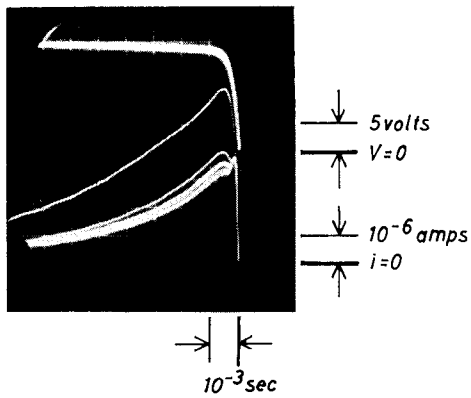

FIG. 4. Transient response characteristic of p-terphenyl under illumination with the band S_1. The time base is 10^{-3} sec/div, and the sweep is from right to left. The upper curve is the voltage trace (5 v/div), and the lower curves are current transients (10^{-6} amp/div) obtained by the procedure described in the text.

absorption in the crystal itself. Both I_0 and I_1 saturate at higher voltages, and the saturation current is also photosensitive.

Crystals of diphenyl and naphthalene were also examined. The currents were always less than 10^{-10} amp for both polarities of the applied voltage, and no photoenhancement was noticed when the acceptor electrode was illuminated with either S_1 or S_2.

B. Transient Current Measurements

The oscilloscope trace photograph of Fig. 4 summarizes the forward current transient measured with a p-terphenyl crystal illuminated in the band S_1. The time base is 10^{-3} sec/div, and the sweep is from right to left. The upper curve is the voltage trace (5 v/div and rise time $\tau_s \simeq 2\times10^{-4}$ sec). The lower curves are transient currents (10^{-6} amp/div) and represent the following experimental procedure. The uppermost current trace is the transient which flows when the voltage is initially applied. If the voltage is then switched off for an interval τ_t of about 10^{-1} sec and then switched on again, the resulting transient is that lying underneath the first. The remaining transients are still smaller and were obtained by successively decreasing the field-off interval below τ_t. The initial transient was always observed after field-off intervals exceeding a few seconds (i.e., appreciably longer than τ_t).

Except for the initial current transient, all the others have 2 maxima, A and B. One maximum (A) peaks at a short time (after a few 10^{-5} sec) and is the same for all field-free intervals, while the other (B) peaks later and decreases with the field-off interval. A detailed analysis of these current transients is given in Appendix A. We show that 2 maxima can occur when the rise time of the voltage τ_s is considerably longer than the time constant τ_c of the circuit. This is the case for the lower current transients of Fig. 4 for which $\tau_s \simeq 2\times10^{-4}$ sec and $\tau_c \simeq (C_m+C_c)R_m = 10^{-5}$ sec. We find that the magnitude and decay time of A are determined by τ_c and τ_s and

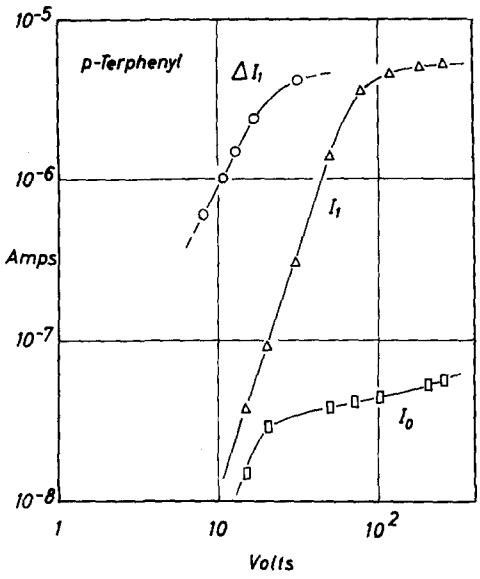

FIG. 5. Forward current-voltage characteristic of *p*-terphenyl. I_0 is the steady-state dark current. I_1 is the steady-state current obtained under illumination with the band S_1, and ΔI_1 represents the voltage dependence of the peak transient-carrier current under the same conditions of illumination.

hence are independent of the field-off interval. The maximum B is due to the flow of holes from the anode into the crystal and is associated with the voltage-dependent resistance R_c of the crystal [see Eq. (2)]. The magnitude of B decreases with the field-off interval because of the space charge of the trapped holes still present from the preceding application of the field. We also show that as maximum B increases, it tends to merge with A to form one maximum. This is the case with the initial current transient. One then obtains B by subtracting A from the total transient.

The maximum B of the initial transient is associated with the flow of holes through the crystal with the traps empty. Its voltage dependence is illustrated by curve ΔI_1 of Fig. 5. The corresponding steady-state current I_1 to which the transients finally decay, and the steady-state dark current I_0 are also shown. ΔI_1 varies with the square of the voltage and tends to saturate at the same current level as I_1.

In Appendix A, we show that maximum A is proportional to the stationary value of the applied voltage [see Eq. (A6)]. Since B can only be measured when it is of the same order or larger than A, our measurements are restricted to the voltage range where this condition is satisfied. The current transients of Fig. 4 were obtained with $R_m = 10^5$ ohms for which the available range is between 7 and 30 v [see curve ΔI_1 of Fig. 5 and Eq. (A6) of the Appendix]. This range can only be extended to lower and higher voltages if maximum A can be reduced [i.e., if the proportionality constant between i_m and $V_{s,0}$ in Eq. (A6) can be made smaller]. Inspection of Eq. (A6) shows, however, that this cannot be easily done. If one increases R_m (i.e., increases the sensitivity of the ammeter), one also increases τ_c [see Eq. (A3)] in the same way so that the height of maximum A remains unchanged. Only by increasing C_m or decreasing C_c (provided $C_m \gg C_c$) or by increasing τ_s can be maximum A be reduced. However, none of these parameters were subject to adjustment in our circuit. Finally, maximum B could also not be measured in the dark because the saturation current was less than maximum A in the voltage range of interest.

IV. DISCUSSION

A. Ohmic Contact

Since one condition for the observation of space-charge-limited current flow in insulators is that at least one contact must be ohmic,[1] the concept of such a contact as it applies to the crystal-electrode system under investigation must be clarified.[11] An ohmic contact gives rise to an excess or reservoir of free carriers in the insulator in the region of the contact. The current through the insulator is then limited by space-charge in its interior and does not depend on the amount of excess charge in the boundary layer so long as there is an excess. If the number of charges supplied by the electrode is insufficient to maintain space-charge-limited current flow, then the contact is no longer ohmic in the above sense, and current saturation may result.[12] Although this concept of an ohmic contact does not require that the motion of injected carriers be described in terms of a band model, the experimental work of Kepler[13] suggests that carrier transport in anthracene can be described in this way. We shall also use this approach in the discussion below.

A saturated solution of iodine in 1.0 M NaI appears to act as an electrode which forms an ohmic contact for hole injection to crystals of those compounds investigated which have more than 2 rings per molecule. Kallmann and Pope[7] have suggested that hole injection takes place when atoms of iodine in solution extract electrons from the valence band of the crystal. Calculations show that an electron gains energy as a result of this transfer. The energy I_A required to remove an electron from the valence band of anthracene to infinity is 5.5 ev,[7] and the energy W_E gained when this electron combines with an atom of iodine in solution to form I^- is 6.2 ev.[7] The energy difference of 0.7 ev gives rise to a transfer of electrons from the valence band of the crystal to the electrode until an equilibrium is attained and leads to the formation of a positive charge layer inside the surface of the crystal in the form of free holes in the valence band. This reservoir of free holes can act as a virtual anode when the injecting

[11] R. H. Bube, *Photoconductivity in Solids* (John Wiley & Sons, Inc., New York, 1960), Chap. 5, pp. 110–128.
[12] R. H. Parmenter and W. Ruppel, J. Appl. Phys. **30**, 1548 (1959).
[13] R. G. Kepler, Phys. Rev. **119**, 1226 (1960).

contact is biased positive. Ohmic contact formation to anthracene is therefore energetically feasible, and the measurements reported here indicate that this is also so with *p*-terphenyl and *p*-quaterphenyl. No hole injection was observed with napthalene and diphenyl. This is not surprising. Since I_A increases with decreasing number of rings in the molecule, it is possible that W_E is less than I_A for diphenyl and naphthalene.

These considerations are sufficient to account for the observed current saturation and for the photosensitivity of the saturation current. The equilibrium concentration of hole donors (atomic iodine in solution) in the acceptor electrode is governed by the reaction[7] I_2 (solution)$\rightleftharpoons 2I$ (solution). The saturation current in the dark is then determined by the thermal equilibrium constant of this reaction. Upon exposing the electrode solution to radiation absorbed by the I_2, the above reaction is shifted to the right, and the concentration of charge donors in the electrode solution is increased. This should not affect the current in the steep portion of the curve; only an *excess* of charge carriers in the boundary layer of the crystal is required to maintain space-charge-limited current flow. However, an increase in this excess means that the steep portion of the curve can now be extended to higher current levels until the electrode is once more exhausted. Hence the saturation current increases with increasing intensity, and the saturation current is related to the absorption spectrum of the acceptor electrode in the way observed.

The slight photosensitivity of the current through *p*-terphenyl and *p*-quaterphenyl in the steep portion of the curve may be explained as follows. The exciting radiation may increase the thickness of the boundary layer and thus increase the current in the steep portion of the curve without affecting its slope [see Eq. (4)]. That the exciting radiation does not affect the slope of the curve is a strong indication that the observed exponent of the power-law between the current and the voltage is a property of the crystal and not of the contact. The strong photosensitivity of the current I_1 through anthracene in the region below saturation is due to the fact that the anthracene crystal itself becomes photoconducting in the band S_1. In addition to being injected at the anode, free holes are also being nonuniformly generated in the bulk of the crystal which contribute to the total current. However, the crystal is transparent enough to the radiation of band S_1 to allow for the excitation of the anode solution and thus the photosensitivity of the saturation current. We shall return to these points later in the discussion.

B. Space-Charge-Limited Currents

1. Steady-State Current

Before discussing the measured current-voltage curves, we outline briefly the germane features of one-carrier space-charge-limited current flow in insulators as developed by Rose[1] and Lampert.[2] Positive holes in excess of the thermal equilibrium density can be injected into a *p*-type insulator through an ohmic anode when the carrier transit time is less than the field-free dielectric relaxation time.[12] This condition can be restated in terms of a threshold voltage above which the injected free-hole density n exceeds the thermal equilibrium density n_0. For a trap-free insulator, the threshold voltage is given by

$$V_i \simeq n_0 e_0 d^2/2\epsilon. \tag{1}$$

(e_0 is the elementary charge, d is the electrode spacing, and ϵ is the permitivity of the insulator.) At voltages less than V_i, the current follows Ohm's law, $j_\Omega = e_0 \mu n_0 V/d$, ($\mu$ is the hole mobility and is assumed independent of the applied field),[14] while above V_i, the current density is limited by the space-charge of the injected holes and follows the relation

$$j_c = (9/8)\mu\epsilon V^2/d^3, \tag{2}$$

which is Child's law for solids.

When traps are present, most of the injected holes may be localized and will not contribute to current flow. As long as $n_0 < n < n_t$ (n_t is the trapped hole density), the magnitude and voltage dependence of the current are dictated by the density and energy distribution of the trapping states. Of particular interest to this discussion is the current-voltage response obtained when the density of trapping states per unit energy range $h(E)$ is approximated by the distribution[15]

$$h(E) = (H/kT_c)\exp(-E/kT_c). \tag{3}$$

(E is the energy measured from the top of the valence band, H is the total trap density, assuming that the distribution holds for all E values above the valence band, and T_c is the characteristic temperature of the distribution greater than the measuring temperature T.) The current-voltage response to which such a distribution leads is given by (see Appendix B)

$$j_t = N_0 \mu e_0^{1-l}\left(\frac{\epsilon l}{H(l+1)}\right)^l\left(\frac{2l+1}{l+1}\right)^{l+1}\left(\frac{V^{l+1}}{d^{2l+1}}\right). \tag{4}$$

(N_0 is the effective density of states in the valence band which has the value 2.4×10^{25} m^{-3} at room temperature and $l = T_c/T$.) The exponent of the voltage in Eq. (4) must always be greater than 2 and becomes larger the more slowly $h(E)$ varies with E. Also derived in Appendix B are the relations for the trapped hole density

$$n_t(x,V) = H\exp(-E_f/kT_c), \tag{5}$$

and the free hole density

$$n(x,V) = N_0\exp(-E_f/kT), \tag{6}$$

[14] For a discussion of the field-dependent mobility, see M. A. Lampert, J. Appl. Phys. **29**, 1082 (1958); and R C A Rev. **20**, 682 (1959).

[15] See also reference 1.

where E_f is the quasi steady-state Fermi level for holes and is given by

$$E_f(x,V)=kT_c \ln\left[\frac{(l+1)^2}{l(2l+1)}\cdot\frac{e_0Hd^2}{\epsilon V}\left(\frac{x}{d}\right)^{l+1}\right]. \quad (7)$$

(x is the distance measured from the anode, and V is the applied voltage.) Lampert[2] has shown that a negligible error is introduced by evaluating E_f at $x=d$ (the cathode), and we shall follow this procedure. Trapping of carriers also increases the threshold voltage to V_{it} which is obtained by solving the equation

$$V_{it}^{l}-V_iV_{it}^{l-1}-V_i\frac{H}{N_0}\left[\frac{(l+1)^2}{l(2l+1)}\cdot\frac{e_0Hd^2}{\epsilon}\right]^{l-1}=0. \quad (8)$$

The current j_t is always less than j_c as long as $n<n_t$. As the voltage is increased, more holes are forced into the solid which distribute themselves among trapping and conducting states in the manner dictated by the distribution (3). Eventually, when n becomes greater than n_t, the current follows Child's law. For the distribution (3), the transition from j_t to j_c occurs at the voltage

$$V_{t-c}\simeq\frac{e_0d^2}{\epsilon}\left[\frac{9}{8}\cdot\frac{H^l}{N_0}\left(\frac{l+1}{l}\right)^l\left(\frac{l+1}{2l+1}\right)^{l+1}\right]^{1/(l-1)}, \quad (9)$$

which reduces to Lampert's formula[2] $V_{t-c}\simeq e_0Hd^2/2\epsilon$ for $l\to\infty$ (i.e., for a uniform distribution of trapped space-charge throughout the volume of the insulator). If the contact is exhausted of carriers before j_t merges with j_c, then j_t merges with the saturation current instead.

2. Transient Current

When a voltage greater than V_i is applied to a p-type insulator with traps which are empty, the initial current due to the flow of holes forced in through the anode is limited only by the space-charge of the mobile holes and obeys Child's law.[1,2] As the free holes are trapped, the current decays to the steady-state value dictated by the density and energy distribution of the trapping states. The decay constant of the current transient is given by the relation

$$\tau\simeq(svH')^{-1}, \quad (10)$$

where s is the capture cross section of the traps, v is the thermal velocity of the free holes (about 10^5 m/sec at room temperature), and H' is the number per m^3 of traps into which the injected holes may decay, which is roughly the number of traps lying above E_f at the voltage applied.[16]

When the voltage is removed, the holes condensed in the traps are thermally released into the valence band and leave the crystal with a relaxation time of the form

$$\tau_t\simeq(1/\nu)\exp(E_f/kT), \quad (11)$$

where E_f is the Fermi-level for holes at the voltage originally applied, and ν is the effective lattice frequency which is related to s through

$$\nu/s=2.5\times10^{30} \quad (12)$$

at room temperature.[17] The relaxation time τ_t can be defined as that time after the voltage is switched off, during which half of the originally trapped charge has been released. If the field is reapplied after an interval appreciably longer than τ_t, the original current transient appears, while for field-off intervals less than τ_t, the space-charge still trapped reduces the initial current below that predicted by Eq. (3).

3. Complete Current-Voltage Characteristic

The idealized complete current-voltage characteristic of an insulator containing traps distributed according to Eq. (3) is summarized by Fig. 6. Below V_i, $n<n_0$; the steady-state current is ohmic (curve j_0), and no transient appears when the field is applied. In the range $V_i<V<V_{it}$, $n<n_0$, but $n+n_t>n_0$; the steady-state current is ohmic, but when the field is applied, a

[16] That H' can be approximated by n_t in Eq. (10) can be seen from the following argument. We can assign a value of E_f to each n [Eq. (6)]. During steady-state current flow the traps above E_f (i.e., those lying at energies $E>E_f$) are practically all filled while those below ($E<E_f$) are practically empty. When the field is first applied, the Fermi level for holes is close to the valence band because of the high free-hole density. Call this value E_f'. Initially all the traps are empty. During the approach to steady state current flow, n becomes smaller, and trapped charges appear although the total charge density remains substantially constant. The traps lying above E_f' are being filled; when they reemit a hole another one is quickly captured, and we can say that holes captured by these traps remain trapped. The traps below E_f' lose holes faster than they can capture them and hence remain, in effect, empty. The Fermi-level for holes moves away from the valence band, and the number of active trapping centers becomes smaller and approaches n_t. Hence, in determining H' we should use an energy between E_f' and the steady-state value E_f in the exponent of Eq. (5). Using the former value instead of the latter increases s by the factor $\exp[(E_f-E_f')]/kT_c$. This factor is about 3 for p-terphenyl (see Sec. V-A) so that s obtained by setting $H'=n_t$ is at most too small by this factor. We must also consider that holes trapped in states between E_f' and E_f are released as the steady state is approached. This increases τ so that the measured τ gives an s value which is too small. This error opposes that introduced by setting $H'=n_t$.

[17] In Eq. (11) we assume that retrapping of holes can be neglected. To justify this, we show that τ_t is much larger than the mean time t_e required for the free holes to flow from the crystal, and thus that the probability w of a trap capturing a hole in the internal t_e is small. To evaluate the lower limit of t_e, we make the assumption that the space charge is homogeneously distributed throughout the crystal during steady-state current flow. For an applied voltage V, the average field inside the crystal after the applied field is switched off is still approximately $F=V/d$. Then t_e is about $\frac{1}{2}$ the transit time or $d^2/2V\mu$. Using the data for p-terphenyl from Sec. V-A, $t_e=2.5\times10^{-5}$ sec or about 4 orders of magnitude smaller than τ_t (10^{-1} sec). The probability $w=vt_esH_{\text{eff}}$, where H_{eff} is the density of trapping centers active for retrapping. Since traps lying more than kT below E_f are occupied for a much shorter interval than the originally filled traps, $H_{\text{eff}}\simeq h(E_f)\cdot kT=n_t(E_f)T/T_c$. Also, since $T_c>T$, it does not matter that the number of traps below E_f is orders of magnitude larger than H_{eff}. Now $n_t(E_f)\simeq V\epsilon/de_0$, so that $w=sv\epsilon T/\mu e_0T_c$ which is a material constant. For p-terphenyl, $w\simeq0.05$ and since this is much smaller than unity, we can use Eqs. (11) and (12) to calculate s.

transient current appears the peak value of which (curve j_c) is trap-free space-charge-limited. It obeys Child's law and hence yields the hole mobility. When $V_{it}<V<V_{t-c}$, $n_0<n<n_t$; the steady-state current (curve j_t) is trap-limited space-charge-limited, and the parameters H and kT_c of the distribution (3) can be obtained from Eq. (4). Finally, when $V>V_{t-c}$, $n>n_t$; the steady-state current is trap-free space-charge-limited, and j_t merges with j_c.

The dashed curve j_s superposed on the current-voltage field is the saturation current which is depicted as being less than the current density where j_t merges with j_c. It arises from the inability of the anode to supply holes to the insulator at an unbounded rate and sets the upper limit on the current which can be drawn through the insulator. Thus the peak transient current and the steady-state current saturate at the same level although the former saturates at a lower voltage than the latter.

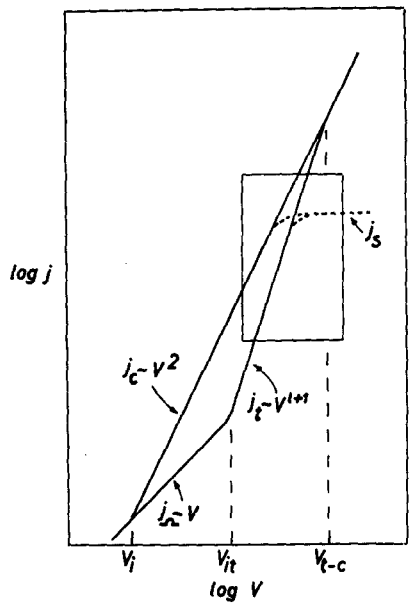

FIG. 6. Complete current-voltage characteristic for space-charge-limited current flow. Below V_{it}, the current follows Ohm's law, j_Ω. Between V_{it} and V_{t-c}, the steady-state current j_t obeys the trap-limited space-charge-limited current relation (4), and above V_{t-c}, the steady-state current follows Child's law, j_c. The peak transient current obeys Child's law for $V>V_i$. j_s is the saturation current. The framed portion corresponds to the measured current-voltage field of Fig. 5.

V. ANALYSIS OF CURRENT-VOLTAGE MEASUREMENTS

A. *p*-Terphenyl

A comparison of the experimental curves of Fig. 5 with the theoretical curves of Fig. 6 shows the following. The measured current-voltage field corresponds to the framed portion of Fig. 6. It falls in the voltage range $V_{it}<V<V_{t-c}$. The experimentally measured peak-transient current ΔI_1 obeys Child's law when the hole mobility is given the value 2.5×10^{-2} cm^2/v sec (using $\epsilon/\epsilon_0=2$). The steady-state currents obey Eq. (4) with $l=2$. Hence the characteristic energy of the distribution (3) is $kT_c=0.05$ ev. Also from Eq. (4) we obtain the value 3.4×10^{16} cm^{-3} for the parameter H. From Eq. (8), $V_{it}=10^{-4}$ v using $n_0\simeq10^4$ cm^{-3} at room temperature,[9] and from Eq. (9), $V_{t-c}=590$ v.

The voltage-dependent parameters have the values $E_f=0.45$ ev, $n=3.5\times10^{11}$ cm^{-3}, and $n_t=4.1\times10^{12}$ cm^{-3} at 80 v, the maximum voltage at which measurements could be made. Since $T_c>T$, Eqs. (5), (6), and (7) are good approximations at room temperature, and we can say that all traps lying above E_f are filled while those beneath are empty. The experimental restriction imposed by the saturation current means that no information can be obtained about the trap distribution for $E<0.45$ ev. The parameter H is therefore only a mathematical value based on the assumption that the distribution (3) holds also in the range between 0.45 ev and the top of the valence band (i.e., that I_1 and ΔI_1 of Fig. 5 can be extrapolated above the saturation current until they meet). Hence Eq. (3) describes the trap distribution for $E>0.45$ ev, and the actual trap density H_t is at least 4.1×10^{12} cm^{-3}.

The theory allows us to calculate the effective lattice frequency ν in two different ways from the transient current measurements: (a) from Eq. (11) using the relaxation time τ_t and (b) from Eqs. (10) and (12) using the decay constant τ. The curves of Fig. 4 were recorded at 20 v for which $E_f=0.52$ ev and $n_t=1.1\times10^{12}$ cm^{-3}. The measured relaxation time is $\tau_t\simeq10^{-1}$ sec. Then from Eq. (11), ν is about 10^{10} sec^{-1}. Alternatively, from Eq. (10) we obtain $s\simeq4\times10^{-17}$ cm^2 using $H=n_t$ at 20 v, $v=10^7$ cm/sec, and $\tau=4\times10^{-3}$ sec, its measured value. With this value of s inserted into Eq. (12), we again obtain $\nu\simeq10^{10}$ sec^{-1}. We consider this agreement as one confirmation of our theoretical interpretation.

The physical parameters of *p*-terphenyl derived above are summarized in the first row of Table I.

B. Anthracene

A similar analysis can also be carried through for our anthracene (see Fig. 3). However, it was not possible to obtain the hole mobility experimentally because meaningful transient-response measurements could not be made. The dark saturation current was too small (less than maximum A of the total transient current), and the current under illumination was probably not solely due to injected holes (see below). We shall therefore set $\mu=1$ cm^2/v sec, a value about that given by Kepler[13] and Boroffka.[8]

The dark current varies as V^{12}. From the equations of Sec. IVB1, we obtain the following: the parameters of the distribution (3) are $kT_c=0.27$ ev and $H=7.6\times10^{13}$ cm^{-3}. At 74 v (the maximum usable voltage), $E_f=0.71$ ev, $n=1.5\times10^7$ cm^{-3}, and $n_t=5.8\times10^{12}$ cm^{-3}.

TABLE I. Summary of results.

	H cm^{-3}	H_t cm^{-3}	kT_c ev	μ cm^2/v sec	S cm^2	ν sec^{-1}
p-terphenyl	3.4×10^{16}	$\leqslant 4.1\times10^{12}$	0.05	2.5×10^{-2}	4×10^{-17}	10^{10}
anthracene	7.6×10^{13}	$\leqslant 5.8\times10^{12}$	0.27	1.0[a]	...	...

[a] Value taken from R. G. Kepler, Phys. Rev. 119, 1226 (1960).

These values are summarized in the second row of Table I.

The current I_1 obtained under illumination is strongly photosensitive at low voltages. We have already mentioned that our anthracene becomes photoconducting when exposed to the bands S_1 and S_2, probably because of absorption by the tetracene impurity. Apparently the free carriers in the crystal due to photoabsorption predominate over the injected carriers at low voltages. As the voltage is increased, the contribution to the total current of the carriers injected from the anode also increases. At a sufficiently high voltage, when the injected carriers predominate, curve I_1 merges with the trap-limited space-charge-limited dark current curve I_0 (that is, with I_0 extrapolated above the saturation level). The curves of Fig. 3 show that this is what would happen if the saturation current were sufficiently large.

One may ask why the current I_1 is not ohmic ($j\sim V$) at low voltages as is the case with CdS under photoexcitation.[3] One reason may be that photoabsorption in most organic photoconductors does not directly give rise to volume-conduction charge. Rather, it is believed that the photon energy is converted into excitons which diffuse through the crystal until they either decay with the emission of fluorescence or until they dissociate into hole-electron pairs at impurity or defect sites and at the surface of the crystal.[2,9,13,18,19] It may also be that the excitons release trapped holes. Under these circumstances, the dark current is space-charge-limited, but below the transition to space-charge-limited current flow, the photocurrent may not necessarily be ohmic.

VI. CONCLUDING REMARKS

The following can be said in support of the contention that the currents measured below saturation are space-charge-limited and that the current carriers are positive holes.

(1) The steady-state current carriers are supplied by the anode and hence are positive holes.

(2) The steady-state current and the peak of the initial transient current saturate at the same current level. This indicates that the transient current carriers are also positive holes supplied by the anode. A current transient would also appear if the action of the field is to draw holes from the insulator faster than they can be replenished at the anode. The peak-transient current then depends on the number of holes (free and perhaps also in states close to the valence band) present in the crystal before the field is applied. The source of carriers for the transient current is then different from the source of the steady-state carriers, and one would not expect both currents to saturate at the same level. Only if the carriers of both currents have a common source should they both saturate at the same level.

(3) The peak-transient current through p-terphenyl varies as the square of the voltage and gives a reasonable value for the hole mobility[20] when fitted to Child's law.

(4) From two independent time-constant measurements (τ_t and τ) and from the assumptions that the steady-state current is space-charge-limited under the influence of an exponential trap distribution and that the hole mobility is field-independent, the effective lattice frequency is obtained in two different ways. These two values of the effective lattice frequency are in good agreement.

Perhaps the strongest argument against the present interpretation is that it requires the assumption of hole trapping states. The literature is devoid of reference to such states. In fact, Moore and Silver[21] have demonstrated that photoexcitation in anthracene produces trapped negative space-charge. Optical absorption leading to photoconductivity gives rise to holes and electrons in equal numbers. Since the hole and electron mobilities are about equal,[13] the trapped negative space-charge and also the p-type photoconductivity generally observed with organic crystals are due to the preferential trapping of electrons.[22] In contrast to this, with the possible exception of the currents through anthracene under illumination, the currents measured here are due to injected positive holes. No photogeneration of carriers occurred in the bulk of the crystals. The density of holes in the crystal is therefore much larger than the electron density, sufficiently so to neutralize any trapped negative space-charge which may be present. That extremely small carrier trap densities (about one part in 10^{12} in our case) can be observed by space-charge-limited current measurements is, as Rose[1] has pointed out, one of the main features of this technique. A direct measurement of the space-charge of the trapped holes is difficult. The simple and elegant procedure of Smith and Rose[3] is not applicable. The space-charge in the crystal must be

[18] D. C. Northrop and O. Simpson, Proc. Roy. Soc. (London) **A234**, 136 (1956); and O. Simpson, Proc. Roy. Soc. (London) **A238**, 402 (1957).
[19] D. Compton, W. Schneider, and T. Waddington, J. Chem. Phys. **27**, 160 (1957).
[20] L. E. Lyons and G. C. Morris, J. Chem. Soc. **1957**, 3648.
[21] W. Moore and M. Silver, J. Chem. Phys. **33**, 1671 (1960).
[22] L. E. Lyon, J. Chem. Soc. **1957**, 5001.

measured with the electrodes removed, and this cannot be easily done with liquid electrodes. Also, the internal polarization technique[21,23] cannot be used because the trapped charge does not perist long enough.

We can say the following about the physical nature of the hole trapping states. Since the lattice sites are occupied by neutral molecules, the trapping centers are also probably neutral when empty. This agrees with the small capture cross section (about 10^{-17} cm^2). For negatively charged centers, the capture cross section would be of the order of 10^{-11} cm^2 at room temperature.[24] The measured capture cross section is also about 100 times smaller than the geometric area of the molecules so that the centers which localize the holes are probably not entire molecules. An exponential energy distribution of trapping states has been suggested for polytetrafluoethylene[25] and CdS,[26] but its physical origin is not clearly understood. However, our knowledge of the distribution is incomplete because our results give no information for the energy range close to the valence band (E less than about 0.5 ev). An acceptor electrode which could deliver holes to the crystal at a rate sufficient to observe the merging of j_t with j_c (Fig. 6) would allow a measurement of the trap distribution to the edge of the valence band.

ACKNOWLEDGMENTS

One of the authors (P. M.) wishes to thank Francis C. Lowell, Jr., of the Polaroid Corporation for many constructive suggestions and for assistance with the experiments.

APPENDIX

A. Analysis of Current Transients

We show that for the circuit described in Sec. II, two maxima can occur in the current transient when the applied voltage $V_s(t)$ rises to its stationary value $V_{s,0}$ with a finite rise time. Assume that $V_s(t)$ rises according to

$$V_s(t)=V_{s,0}(1-e^{-t/\tau_s}). \tag{A1}$$

For the voltage trace of Fig. 4, the time constant τ_s of the voltage source is about 2×10^{-4} sec and $V_{s,0}=20$ v. The differential equation for the current i_m through the resistance R_m of the ammeter is

$$\frac{di_m}{dt}=-\frac{i_m(t)-i_{m,\mathrm{stat}}(t)}{\tau_c}+\frac{1}{R_m}\left(\frac{C_c}{C_c+C_m}\right)\frac{dV_s}{dt}, \tag{A2}$$

where

$$\tau_c=(C_c+C_m)\Big/\left(\frac{1}{R_c}+\frac{1}{R_m}\right)$$

$$\simeq(C_c+C_m)R_m=10^{-5}\text{ sec} \tag{A3}$$

and

$$i_{m,\mathrm{stat}}(t)+V_s(t)/(R_c+R_m). \tag{A4}$$

We note that $\tau_c/\tau_s=1/20$ and consider two limiting cases: (a) $t\ll\tau_s$ and (b) $t\ll\tau_c$.

(a) $t\ll\tau_s$

For $t\ll\tau_s$, the solution of Eq. (A2) can be written as

$$i_m(t)=\frac{C_c}{C_c+C_m}\cdot\frac{V_{s,0}}{R_m}\cdot\frac{\tau_c}{\tau_s}(e^{-t/\tau_s}-e^{-t/\tau_c}). \tag{A5}$$

Hence i_m rises with the time constant τ_c to the value

$$i_m(t_{\max})\simeq\frac{C_c}{C_c+C_m}\cdot\frac{V_{s,0}}{R_m}\cdot\frac{\tau_c}{\tau_s}\left[\left(\frac{\tau_c}{\tau_s}\right)^{(\tau_c/\tau_s)}-\frac{\tau_c}{\tau_s}\right]$$

$$[\simeq4\times10^{-6}\text{ amp}]. \tag{A6}$$

The time at which this maximum occurs is

$$t_{\max}=\tau_c\ln\tau_s/\tau_c[\simeq3\times10^{-5}\text{ sec}]. \tag{A7}$$

We note that $i_m(t_{\max})$ is proportional to $V_{s,0}$. To the right of the maximum, i_m decays to zero with the longer time constant τ_s. The peak, Eq. (A6), of i_m is associated with the first maximum (A) of the lower current transients of Fig. 4. This maximum occurs after a few 10^{-5} sec and corresponds to an i_m of 4×10^{-6} amp. We note the good agreement with the values calculated from Eqs. (A6) and (A7) which are shown in parenthesis after each equation. We have used $C_c=C_m\simeq10^{-10}$ farads and $R_m(\ll R_c)=10^5$ ohms (see Sec. II and the discussion of Figs. 4 and 5). The maximum of i_m is the same for all the lower current transients because these were all recorded with $V_{s,0}=20$ v.

(b) $t\ll\tau_c$

From Eq. (A2) and directly from Fig. 4, it can be shown that

$$R_m|di_m/dt|\ll dV_s/dt, \tag{A8}$$

at least in the region between the two maxima. Hence the solution of Eq. (A2) becomes

$$i_m(t)=\frac{V_{s,0}}{R_m+R_c}(1-e^{-t/\tau_s})+\frac{C_c}{C_c+C_m}\cdot\frac{\tau_c}{\tau_s}\cdot\frac{V_{s,0}}{R_m}e^{-t/\tau_s}. \tag{A9}$$

i_m still rises with the time constant τ_c to the maximum given by Eq. (A6), but now decays with the longer time constant τ_s to the value $V_{s,0}/(R_m+R_c)$ instead of zero.

We now consider the voltage dependence of the crystal resistance R_c which has the form [see Eq. (2)]

$$R_c(t)=[\alpha/V_s(t)], \tag{A10}$$

where α is a constant. Here we have used $V_s(t)$ instead of $V_c(t)$, the voltage drop across R_c, because these two voltages are practically the same when $R_m\ll R_c$. The

[23] H. Kallmann and B. Rosenberg, Phys. Rev. **97**, 1596 (1955).
[24] See reference 11, p. 61.
[25] J. F. Fowler and F. T. Farmer, Nature **174**, 136 (1954).
[26] A. Rose, R C A Rev. **12**, 362 (1951).

solution of Eq. (A2) is now

$$i_m(t)=\frac{V_s(t)}{R_m+[\alpha/V_s(t)]}+\frac{C_c}{C_c+C_m}\cdot\frac{\tau_c}{\tau_s}\cdot\frac{[V_{s,0}-V_s(t)]}{R_m} \quad \text{(A11)}$$

for $t\gg\tau_c$. This function does not monotonically approach a stationary value. Rather, it has a minimum after the first maximum Eq. (A6) as can best be seen by differentiating with respect to V_s. i_m goes through a minimum when $V_s(t)=V_s^*$, where

$$V_s^*=\frac{\alpha}{2R_m}\cdot\frac{\tau_c}{\tau_s}\cdot\frac{C_c}{C_c+C_m}. \quad \text{(A12)}$$

After passing through the minimum, $i_m(t)$ rises again and approaches the value $i_{m,\mathrm{stat}}(\infty)$ [Eq. (A3)] with R_c given by Eq. (A10) also at $t=\infty$. However, because of trapping, i_m may not actually reach $i_{m,\mathrm{stat}}(\infty)$, but rather may go through a second maximum and decay to the stationary value given by Eq. (4) (or curve I_1 of Fig. 5) with the time constant associated with the trapping of carriers in the crystal [see Eq. (10)].

A brief numerical substitution will demonstrate the quantitative agreement between this analysis and the curves of Fig. 4. From the location of the minimum, we obtain V_s^* and from Eq. (A12), α. With this α, we obtain $R_c(t)$ vs $V_s(t)$, and from $V_s(t)$ at the second maximum, we obtain $R_c(\mathrm{min})$, the minimum value of R_c. From the largest transient displaying two maxima, $R_c(\mathrm{min})\simeq 5\times 10^6$ ohms $\gg R_m$. Alternatively, from $i_m(t)$ at the second maximum, we can also obtain $R_c(\mathrm{min})$ directly from Eq. (A5) (which is a good approximation at this time). We again obtain $R_c(\mathrm{min})\simeq 5\times 10^6$ ohms. This is an excellent verification of the validity of Eqs. (A10) and (2).

Finally, we treat the question: Why does the initial current transient of Fig. 4 exhibit no minimum? This transient was measured after the crystal had been left without an applied field for a time sufficient to allow all the space-charge in the crystal to flow out. In this case, the largest number of current carriers can enter the crystal when the voltage is again applied. The condition $R_c=\alpha/V_s$ is best satisfied, and α is smaller than for the other transients. Because of Eq. (A12), V_s^* becomes smaller with α. This means that the minimum moves closer to the first maximum. The condition $t\gg\tau_s$, which is already not ideally satisfied by the lower transients, is then even less satisfied by the initial transient. One must expect, therefore, that the first and second maxima combine into a single maximum. This is the case for the initial transient. For the remaining transients, however, α gets larger as the field-off interval is shortened, and so V_s also becomes larger at the minimum of each curve. Hence the minima should appear at successively later times. This is also shown by Fig. 4. But the first maximum (A), which depends only on the stationary value of V_s and the voltage-independent circuit parameters [Eq. (A6)], must be the same for all the transients displaying two maxima since these were all recorded at 20 v. This is also clearly demonstrated by Fig. 4.

B. Mathematical Formulation

The following calculations are based on the assumptions that the hole mobility is field-independent, and that the density of hole trapping states per unit energy range $h(E)$ above the valence band is described by the distribution

$$h(E)=(H/kT_c)\exp(-E/kT_c), \quad \text{(B1)}$$

where E is the energy measured upward from the top of the valence band, H is the total trap density, and T_c is a characteristic constant of the distribution. We also assume for the moment that the absolute temperature $T=0$, and that the positive space-charge $\rho(x)$ at the distance x from the anode fills all the traps to a quasi Fermi level for holes $E_f(x)$. Then

$$\rho(x)=e_0\int_{E_f(x)}^{\infty}\frac{H}{kT_c}e^{-E/kT_c}dE=(e_0H)\exp(-E_f(x)/kT_c), \quad \text{(B2)}$$

where e_0 is the elementary charge. The upper limit of the integral has been extended to infinity. This is permissible provided that $E_f(x)$ is far enough removed from the Fermi level of the neutral crystal. If we now raise the temperature and assume that a Fermi distribution for the injected holes has been established for all x, the new quasi Fermi level will not differ significantly from that defined by Eq. (B2) if $T_c>T$ and if $\rho(x)>\rho_f(x)$, the density of free charge in the valence band. If $E_f(x)\gg kT$, then $\rho_f(x)$ is given by

$$\rho_f(x)=(N_0e_0)\exp(-E_f(x)/kT), \quad \text{(B3)}$$

where N_0 is the effective density of states in the valence band. From Eqs. (B2) and (B3) we obtain the relation between the free and the total charge density

$$\rho_f(x)=N_0e_0^{1-l}H^{-l}[\rho(x)]^l, \quad \text{(B4)}$$

where $l=T_c/T$.

We seek a solution for the equations

$$dF/dx=\rho(x)/\epsilon \quad \text{(B5)}$$

and

$$j_t=\mu\rho_f(x)F(x), \quad \text{(B6)}$$

subject to the boundary condition $F(0)=0$. Here $F(x)$ is the electric field strength, j_t is the current density, ϵ is the permitivity of the crystal, and μ is the hole mobility. We have neglected the diffusive contribution to the total current (see Appendix C). From Eqs. (B4),

(B5), and (B6) we obtain

$$dF/dx = D[F(x)]^{-1/l},$$

where

$$D = (H/\epsilon)e_0^{(l-1)/l}(j_t/N_0\mu)^{1/l}.$$

The solution satisfying the boundary condition is

$$F(x) = \left(\frac{l+1}{l}D\right)^{l/(l+1)} x^{l/(l+1)}. \quad \text{(B7)}$$

To obtain the potential, we integrate Eq. (B7) from $x=0$ (anode) to $x=d$ (cathode) and obtain

$$V = \left(\frac{l+1}{l}D\right)^{l/(l+1)}\left(\frac{l+1}{2l+1}\right)d^{(2l+1)/(l+1)}.$$

Substituting for D and solving for j_t, we have

$$j_t = N_0\mu e_0^{1-l}\left(\frac{\epsilon l}{H(l+1)}\right)^l\left(\frac{2l+1}{l+1}\right)^{l+1}\frac{V^{l+1}}{d^{2l+1}} \quad \text{(B8)}$$

which is Eq. (4) of the text.

When no traps are present, the current density follows Child's law for solids,

$$j_c = (9/8)\mu\epsilon V^2/d^3. \quad \text{(B9)}$$

By setting j_t equal to j_c, we obtain the transition voltage V_{t-c} [Eq. (9)] from trap-limited to trap-free space-charge-limited current flow

$$V_{t-c} = \frac{e_0d^2}{\epsilon}\left[\frac{9}{8}\cdot\frac{H^l}{N_0}\left(\frac{l+1}{l}\right)^l\left(\frac{l+1}{2l+1}\right)^{l+1}\right]^{1/(l-1)}, \quad \text{(B10)}$$

which reduces to Lampert's formula[2] $V_{t-c}=e_0Hd^2/2\epsilon$ for $l\to\infty$; that is, when the trap distribution is uniform and when the current-voltage curve j_t vs V becomes infinitely steep. The total trap density can now be obtained in two ways. Solving Eq. (B8) for H yields

$$H = \frac{\epsilon l}{l+1}\left[\frac{N_0\mu}{j_te_0^{l-1}}\left(\frac{2l+1}{l+1}\right)^{l+1}\frac{V^{l+1}}{d^{2l+1}}\right]^{1/l}. \quad \text{(B11)}$$

Alternatively, if the transition voltage V_{t-c} can be measured, we can solve Eq. (B10) for H and obtain

$$H = \frac{l}{l+1}\left(\frac{\epsilon V_{t-c}}{e_0d^2}\right)^{(l-1)/l}\left[\frac{8N_0}{9}\left(\frac{2l+1}{l+1}\right)^{l+1}\right]^{1/l}, \quad \text{(B12)}$$

which is independent of μ and j_t.

Finally, we obtain for the quasi Fermi level for holes the relation

$$E_f(x) = kT_c\ln\left[\frac{(l+1)^2}{l(2l+1)}\cdot\frac{e_0Hd^2}{\epsilon V}\left(\frac{x}{d}\right)^{l+1}\right], \quad \text{(B13)}$$

by differentiating Eq. (B7) and substituting into Eq. (B2).

C. Estimation of the Diffusion Current in Relation to the Field-Driven Current

To estimate the importance of the diffusive contribution to the total current density, we consider the equations

$$j_{\text{field}} = \mu\rho_fF$$

and

$$j_{\text{diff}} = -D(d\rho_f/dx),$$

where j_{field} is the field-driven current density, j_{diff} is the diffusion current density, and D is the diffusion constant for holes. Using the Einstein relation $D=\mu kT/e_0$, we obtain the ratio

$$\left|\frac{j_{\text{diff}}}{j_{\text{field}}}\right| = \frac{kT}{e_0F}\cdot\frac{1}{\rho_f}\cdot\frac{d\rho_f}{dx}.$$

From Eqs. (B5) and (B7) we find that

$$\rho_f(x)\sim x^{-l/(l+1)}$$

so that

$$\frac{1}{\rho_f}\cdot\frac{d\rho_f}{dx} = -\frac{l}{l+1}\cdot\frac{1}{x}$$

and

$$\left|\frac{j_{\text{diff}}}{j_{\text{field}}}\right| = \frac{kT}{e_0F}\cdot\frac{l}{l+1}\cdot\frac{1}{x}.$$

Hence the diffusion current predominates in the vicinity of the anode. Further into the crystal, however, the reverse is true. For instance, for a 50-μ thick crystal and a potential of only 2 v

$$\left|\frac{j_{\text{diff}}}{j_{\text{field}}}\right| < 0.1$$

for $x=5\,\mu$. The situation becomes still more favorable at higher voltages. These considerations serve as a justification for neglecting the diffusion current in the derivations of Appendix B.